UNDERSTANDING STRENGTH AND MICROSTRUCTURE OF SGA USING NANOINDENTATION AND ULTRASOUND TESTING

H. Wijayaratne[1*], L. Perander[2], M. Hyland[1], J. Metson[1], D. Framil Carpeño[3]

[1] *Light Metals Research Centre, The University of Auckland, Auckland, New Zealand*

[2] *Outotec GmbH, Oberursel, Germany*

[3] *Department of Chemical and Materials Engineering, The University of Auckland, Auckland, New Zealand*

Corresponding author: h.wijayaratne@auckland.ac.nz

ABSTRACT

The strength of agglomerated particles of Smelter Grade Alumina (SGA) is a very important property as it indirectly impacts on how the material behaves during handling, transportation, storage and ultimately feeding to aluminium reduction cells. Poor strength, contributes to the generation of fines as a result of particle breakdown. The level of fines in alumina impacts on the working environment through the formation of dust as well as on the cell operation. Eventually this leads to poor pot line performance and increased emissions.

Determination of an industrially relevant measurement of alumina strength is a considerable challenge. The Forsyth-Hertwig method, which is well established in the industry, has many limitations. One of the main limitations is the fact that it is an aggressive test and evaluates only the <45 µm fraction which easily leads to a perceived attrition strength that is inaccurate. Thus the development of a measurement of true particle strength is of value for the industry as well as for fundamental understanding of alumina microstructure and particle strength. This paper reports on experimental investigations of industrial SGAs and laboratory prepared samples to explore alumina particle strength using nanoindentation as well as ultrasound mediated particle breakage tests. These techniques demonstrate the influence of alumina microstructure on its apparent strength and provide insights into the evolution of strength within alumina particles in the calcination process.

1. INTRODUCTION

Although alumina strength is a popular subject of discussion in terms of attrition and fines generation, there appears to be no working definition of what is meant by true alumina or gibbsite strength (Chandrashekar et al. 2005). This is partly because of the well-established convention of focusing on the amount of fines as an indication of strength and the difficulties of measuring alumina strength in a way that is more fundamental as well as industrially relevant.

A considerable amount of previous research has been carried out in understanding alumina strength. Most of this has been in terms of alumina and hydrate attrition strength as measured by the standard Forsyth-Hertwig test (Anjier and Marten 1982, Clerin and Laurent 2001, Stählin et al. 1985, Sang 1987 and Yamada et al. 1983). The main limitation with the attrition index as measured by the Forsyth-Hertwig method is, its dependence on the initial particle size distribution of the test sample (Clerin and Laurent 2001). This could easily lead to weak aluminas being perceived as strong and vice versa since only the change in minus 45 µm fraction before and after the test is evaluated.

To overcome this, a handful of studies have been done on developing novel methods to measure and understand breakage behaviour of aluminas (Audet and Clegg 2011, Coghill and Giang 2011, 2008, Ilievski et al. 2005, Kristiansen et al. 2012). However many questions still remain unanswered and the most fundamental of these include ‘what is defined as alumina strength?’ and ‘how does this strength evolve as a function of microstructure or as a function of calcination?’ In particular, the broad underlying research interest that forms the basis of this study is to understand how strength relates to microstructure in terms of phase distribution and local impurity distributions within particles. This is a complex problem since there is clear

evidence (Perander et al. 2011) that even a single particle of alumina is heterogeneous in nature.

A powerful tool such as nanoindentation has the capability to probe the microstructure with good spatial resolution, allowing the possibility of studying the mechanical properties of a material at a very small scale. This is ideal for a complex multiphase material such as alumina, since understanding the variation in mechanical properties of even a single particle is achievable. Furthermore, when used together with other microscopy techniques (such as ESEM and TEM) and impurity mapping techniques such as Nano-SIMS, linking the mechanical property distributions of a particle to its variation in microstructure becomes a possibility.

This paper explores nanoindentation as a technique to study the properties of alumina (laboratory calcined and industrially calcined) at the nanoscale which gives some important considerations on how strength might be defined and how it evolves with calcination. Furthermore, this work looks at the development of a particle breakdown test using ultrasound as an alternative method that maybe used to study particle breakdown.

2. NANOINDENTATION TESTING

Nanoindentation testing carried out in this study was conducted using a Hysitron TI-950 Triboindenter with a standard Berkovich tip. All alumina samples tested were embedded in epoxy resin, ground and manually polished down to a final surface finish of 1µm.

2.1 Nanoindentation Theory

During nanoindentation, both the applied force and resultant displacement are recorded simultaneously while a rigid indentation tip is pushed into the material of interest (Dickinson and Schirer 2009). The forces/load applied during nanoindentation can be chosen to reflect the properties of the material being tested. Throughout this study, alumina particles were indented at a maximum load of 2000µN and 4000µN.

The output of the nanoindentation test is a load-displacement curve which is characteristic of the behaviour of the material being tested (Figure 1 provides an example). These curves contain a rich source of information showing ductility or brittleness, dislocation motion and creep behaviour (Dickinson and Schirer 2009). Nanoindentation data analysis consists of specifically analysing the unloading data (unloading part of the curve) assuming that this data arises from purely elastic contact. The Oliver-Pharr method is widely accepted and used for analysis of elastic-plastic indentation data (Oyen and Cook 2009).

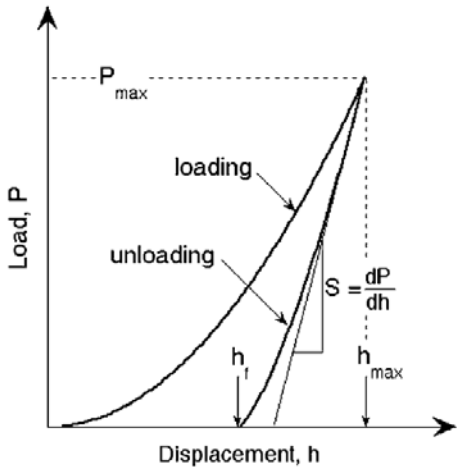

Figure 1. An example of indentation load-displacement data showing important measured parameters (Oliver and Pharr 1992)

In the Oliver-Pharr method, the unloading part of the load-displacement curve is described by a simple power law (equation 1) with fitting parameters α and m where ($h-h_f$) describes the elastic displacement of the indenter tip (Oyen and Cook 2009, Oliver and Phaar 2004,).

$$P = \alpha(h - h_f)^m \qquad (1)$$

From these parameters, the stiffness (S = dP/dh) at peak load is determined and contact depth (h_c) is computed from the stiffness at peak load using equation (2) where β (≤ 1) is a dimensionless geometry parameter related to the shape of the probe (typically accepted to be 0.75 for a paraboloid of revolution).

$$h_c = h_{max} - \beta \frac{P_{max}}{S} \qquad (2)$$

Determination of the contact depth allows the derivation of an 'area function' which describes the projected area of the indenter at contact or contact area. The area function is carefully calibrated using a

standard fused quartz sample, and it also accounts for non-ideal tip geometries arising from tip rounding etc. (due to wear).

$$A = F(h_c) \qquad (3)$$

Measurement of the indentation elastic modulus is possible from its relationship with contact area and measured unloading stiffness through equation (4).

$$E_R = \frac{S\sqrt{\pi}}{2\sqrt{A}} \qquad (4)$$

Contact hardness (H_c) is determined by dividing the peak load (P_{max}) by the contact area (A_c).

$$H = \frac{P_{max}}{A_c} \qquad (5)$$

However, it must be remembered that the Oliver and Pharr analysis is valid for materials that depict ideal elastic-plastic behaviour as shown in the Figure 1. Care must be taken when applying this method to materials such as gibbsite which show non-ideal (elastic-plastic behaviour) force-displacement curves as will be discussed below.

3. RESULTS AND DISCUSSION

In this study, attempts have been made to characterise gibbsite, SGA's as well as laboratory calcined alpha alumina (prepared from a Bayer gibbsite precursor by heat treatment in a muffle furnace at 1100°C for 96hrs) using nanoindentation and ultra-sonication. The main objectives of this work have been two-fold: (i) to study the variation in mechanical properties of a single particle of these three distinct materials and (ii) to gain an understanding of how strength varies during the calcination/de-hydroxylation process. Furthermore, where data has been available, attempts have been made to compare nanoindentation result outcomes with industrial attrition strength measurements.

3.1 Force-displacement Curves

Force-displacement curves obtained with gibbsite, SGA and laboratory calcined alpha alumina are considerably different and can be considered characteristic of each type of material in how each responds to the application of load. Figure 2 depicts the three types of force-displacement curves observed.

Gibbsite demonstrates 'pop-in' events during loading which are usually related to dislocation motion (Kelchner et al. 1998), slip band formation (Bradby et al. 2001) or cracking events (Scholz et al. 2004). However in this instance, it is speculated that these 'pop-ins' are linked to the mechanical response of the layered structure in gibbsite to the applied load. Laboratory calcined alpha alumina demonstrate uneven loading curves where the changes in the loading part of the curves are more 'smooth' without 'sharp' changes as observed in gibbsite curves. Moreover, the initial portions of the laboratory calcined alpha curves have a very small slope after which they increase. This period of low initial slope is indicative of a false tip contact, which could be attributed to a high roughness of the specimen. Although roughness is related to specimen preparation, it must be noted that all samples tested were subjected to the same sample preparation (i.e. in terms of grinding and polishing stages). Hence, the roughness observed with the alpha alumina maybe assumed to be more inherent than externally caused.

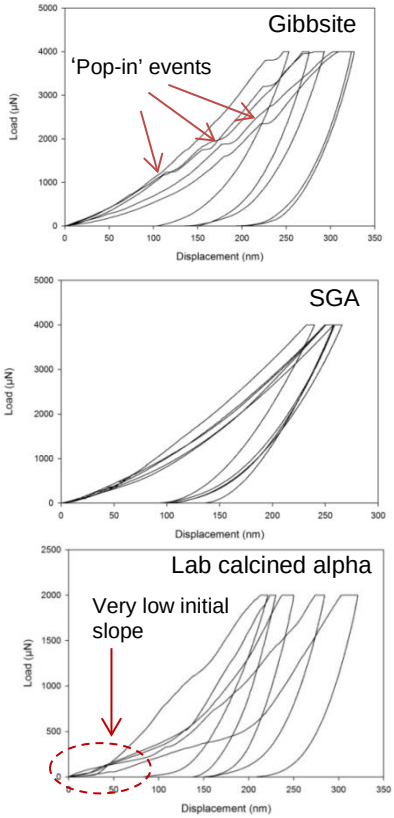

Figure 2. Examples of typical force-displacement curves obtained for gibbsite, SGA and laboratory calcined alpha alumina

This is also evident in ESEM images obtained on the laboratory calcined alpha alumina sample as presented in Figure 3 showing a very rough/porous structure.

Only the SGA force-displacement curves show consistent elastic-plastic behaviour where Oliver-Pharr method can be accurately applied for analysis to determine hardness and modulus data.

In contrast, although the unloading response of gibbsite and laboratory calcined alpha alumina appear to be elastic and consistent; applying the Oliver and Pharr method to determine hardness and modulus would yield unrealistic values since these properties depend on A_c that is a function of contact depth h_c (Equations 4 & 5) which in turn cannot be determined accurately from non-ideal curves.

At best the hardness and modulus data obtained in these instances can be referred to as 'apparent'. Hence, stiffness (S) or the slope of the unloading curve is a more appropriate measure of material's strength under these circumstances assuming that the underlying mechanisms which operate during the pop-ins do not affect the unloading part of the curves.

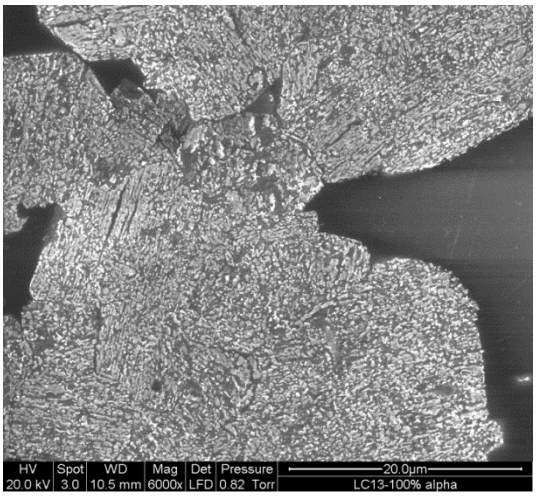

Figure 3. ESEM charge contrast image of laboratory calcined alpha alumina showing rough/porous microstructure.

3.2 Stiffness of Individual Particles

Individual particles of gibbsite, SGA and laboratory calcined alpha alumina samples have been tested by imaging and indenting whole particles less than approximately 50 µm in diameter. This small size was selected due to the time consuming nature of the tests and a maximum of two particles each were tested during this study. The purpose of this was to understand the variation of mechanical properties of a single particle across its cross section and observe the differences in properties of the epoxy resin and particle. An example of a stiffness map (depicted as a contour plot) generated using the x, y coordinates of each indent and corresponding stiffness values for a gibbsite particle is given in Figure 4. A Scanning Probe Microscope (SPM) image of the corresponding gibbsite particle prior to indentation is presented in Figure 5. The contour plot clearly shows the perimeter of the particle where the stiffness of the epoxy resin is lower (blue) compared to the bulk of the particle. The two red regions depict 'hot spots' of apparent high stiffness regions within the particle. By studying Figure 5, it is clear that these are in fact areas of the particle that appear to have cracked or contain discontinuities. Apart from these spots (artefacts) and the edges of the particles where the indentations would have occurred at the particle-epoxy interface, the stiffness of the middle of the particle is more or less uniform and predominantly in the range of 50-60 N/nm.

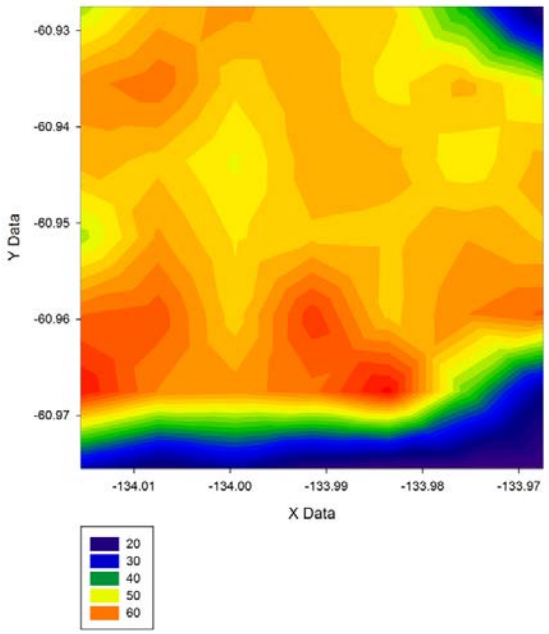

Figure 4. Gibbsite single particle contour plot of stiffness. X and y data represent x and y coordinates. Scan size (60 x 60 µm). Indents were made as an array of 7x7 with a separation of 8µm between indents. A maximum load of 2000µN, was applied for each indent

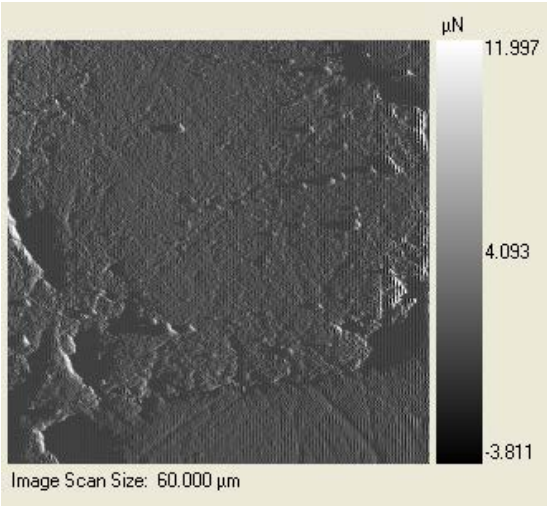

Figure 5. SPM image of the Gibbsite particle tested as presented in Figure 4

The stiffness data generated by the same method for SGA and laboratory calcined alpha particles is plotted together with that of gibbsite in Figure 6, while the mean stiffness data are given in Table 1. Figure 6 and Table 1 demonstrate the variation in stiffness of individual species even across only two individual particles. However, very low stiffness values should be disregarded as they represent the softer epoxy resin that is surrounding the particles. Moreover, the variation within each sample is likely due to many factors such as orientation of crystals, defects such as roughness/porosity as well as phase distributions (in SGA) etc. The most evident conclusion that can be drawn from Figure 6 is that although the stiffness of gibbsite appears to be higher and statistically different (statistical analysis not reported here) from both SGA and laboratory calcined alpha alumina; the stiffness of the latter two materials' overlap. This could be due to the presence of some alpha alumina (~10 wt% as determined by phase quantification using Rietveld refinement on XRD data - not included in this paper) in this particular SGA as well as other factors as mentioned. Thus, since SGAs are quite similar in phase distributions, nanoindentation technique is expected to give similar mechanical property data between them except during instances where the SGAs being tested are known to have significantly different strengths (i.e. as given by attrition index). However the problem lies in not having a measure of 'true' alumina strength since attrition index is known to have many limitations, as exemplified in testing the industrial SGAs in this study.

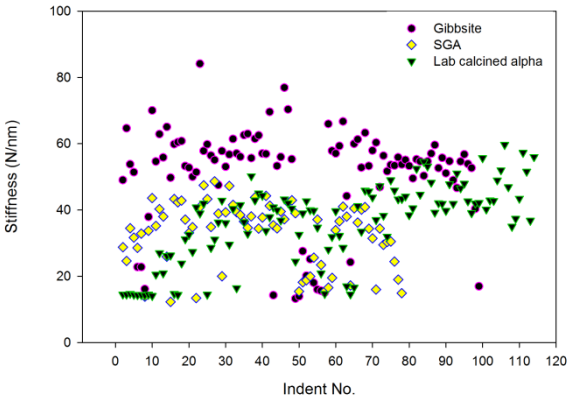

Figure 6. Extent of variation in stiffness across gibbsite, SGA and laboratory calcined alpha particles. Data from two individual particles of each species is presented. By performing a Kruskal-Wallis ANOVA analysis (Dunn's method) the population of stiffness data of gibbsite was confirmed to be statistically different to that of SGA and laboratory calcined alpha

Table 1: Mean and standard deviation data for the samples presented in Figure 6

Sample	Mean Stiffness (N/nm)
Gibbsite	50.81 ± 15.23
SGA	32.88 ± 9.60
Laboratory calcined alpha alumina	36.21 ± 11.86

3.3. Industrial Sample Testing

Three industrial SGA samples with known average approximate attrition strengths were tested using nanoindentation and the mechanical property data are presented in Figure 7 and Table 2. The mechanical property data obtained indicate that these three samples are not drastically different as indicated by the attrition indices. From the indentation data, SGA 1 & 2 can be considered quite similar with comparable strengths; with SGA 3 being somewhat weaker. Thus it is not possible to reconcile these observations with the attrition strength measurements that are known to be unreliable due to the nature of the Forsyth-Hertwig test and the attrition indices presented being not precisely of the sample tested (i.e. averaged historical data and CoA data both of which could be variable depending on a particular shipment). Furthermore it is to be noted that the tests carried out here are based on a very small number of particles since the purpose of this study was to conduct a

proof-of-concept experiment to observe any detectable differences between SGAs rather than establish a statistically robust experimental method.

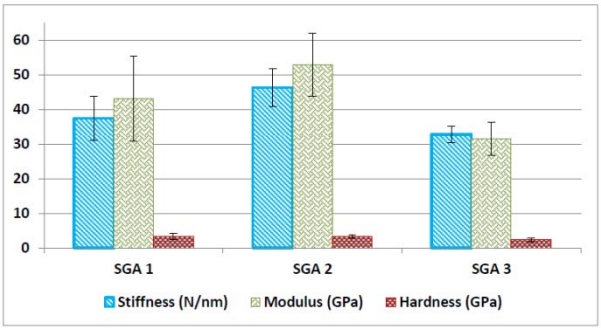

Figure 7. Indentation mechanical property data obtained for three industrial SGAs

Table 2. Measured data for sample presented in Figure 7

	Stiffness (N/nm)	Modulus (GPa)	Hardness (GPa)	Attrition Index
SGA 1	37.3 ± 6.4	42.9 ±12.2	3.3 ± 0.9	4.5
SGA 2	46.3 ±5.4	52.9 ± 9.1	3.3 ± 0.5	13
SGA 3	32.8 ± 2.4	31.5 ±4.8	2.4 ± 0.5	48

4. ULTRASOUND MEDIATED PARTICLE BREAKAGE

The difficulty in this study in making direct comparisons between attrition strength measurements and nanoindentation data on the small number of samples examined here has prompted the investigations of another particle breakage test method using ultrasound. Preliminary work conducted in developing this test will be summarised for the purposes of this paper.

Fragmentation of agglomerates using high intensity ultrasound waves is a known phenomenon which has been studied with regard to size reduction and improving sinterability of ceramic powders (Kass 2000, Kuster et al. 1993). Agglomerates are known to break up during sonication due to interaction with collapsing cavities in the liquid.

4.1 Ultrasound Test Method

Sonication treatment of SGAs has been carried out in this work using a Hielscher UPS200S ultrasound probe fitted with the S3 type sonotrode. This particular sonotrode has power density and maximum amplitude specifications of 460 W/cm^2 and 210µm respectively. For this work, the probe was operated at its 100% amplitude setting with the aim to cause maximum particle breakage.

The basic procedure consisted of alumina samples (~1.5g) being immersed in a beaker of water and sonicating for set a duration. Afterwards the contents of the beaker including the sonicated particles are introduced into a laser particle size analyser for post particle size analysis. For comparison, the samples subjected to treatment need to be tested for particle size distribution without any sonication treatment as well.

4.1.1 Laser particle size analysis

Particle size analysis has been carried out using a Malvern Mastersizer 2000 unit (with a size range capability of 0.02 – 2000 µm). This measurement is based on laser diffraction which relies on the fact that particles passing through a laser beam scatters light at angles related to their size (Kippax 2005, Malvern Instruments). The scattering intensity also depends on particle size, reducing with particle volume. Hence large particles scatter light at narrow scattering angles with high intensity while small particles scatter light at wide angles with low intensity. The Mastersizer unit consists of a laser beam with a fixed wavelength, a series of detectors to measure light patterns of a wide range of angles and a sample dispersion unit to ensure particles being measured passes through the laser beam in a homogeneous well dispersed stream. Once the system captures the scattering patterns of the test sample, the particle size distribution is calculated by comparison of these patterns with a suitable optical model – i.e. in this case the *Mie theory* which predicts how light scatters from solid particles (transparent or opaque) with the assumption that particles are spherical. It is also required that the refractive indices of both the sample and the dispersion medium as well as the absorption coefficient of the sample are known or estimated. In this study, the refractive index of alumina is used as 1.78 and the absorption is estimated at 0.1 (from the inbuilt database within the unit software). At this stage, these properties are assumed to be reasonably constant for

different aluminas tested. However, it has been noted that when a large amount of fines are present in a sample during measurement, the fit between the scattering pattern and the optical model is not ideal and hence, optimisation of the method is required (as part of ongoing development) for measurement of aluminas particularly after sonication treatments.

4.2 Preliminary Results

Preliminary work has been conducted on a standard industrial SGA sample that was sonicated for durations of 5 minutes and 10 minutes immersed in 50 ml and 100 ml of water respectively. From the post-treatment particle size analysis carried out, it was observed that the most noticeable amount of particle breakage has occurred with sonicating in 50 mL for duration of 10 minutes. The particle size distribution data of the samples tested compared to untreated sample is presented in Figure 8. The untreated sample particle size distribution has been measured three times and the reproducibility of the laser measurement is indicated with the corresponding measurement. It is clear that sonicating in 50 mL volume for 10 minutes gives a significant particle size distribution change compared to the measurement error/variability. Thus, these operating conditions are chosen as satisfactory conditions for particle breakage tests.

The extent of particle breakage however needs to be defined with care. This is to avoid focussing only on the extent of fines generated since that depends on the extent of large particles present initially. Furthermore, there could be instances where although fines are generated, these get agglomerated during post treatment particle size testing or handling. Thus, particle breakage needs to be scrutinised at individual particle size fractions to obtain an overall 'breakage factor'. Development of this technique is on-going and a large number of samples with varying strengths need to be tested in order to determine the best method of quantifying such a breakage factor. Furthermore, since the quantification of breakage is highly dependent on the laser particle size measurement, the influence of all factors that could affect the measurement; particularly for aluminas with varying quantities of fines needs to be verified to improve accuracy.

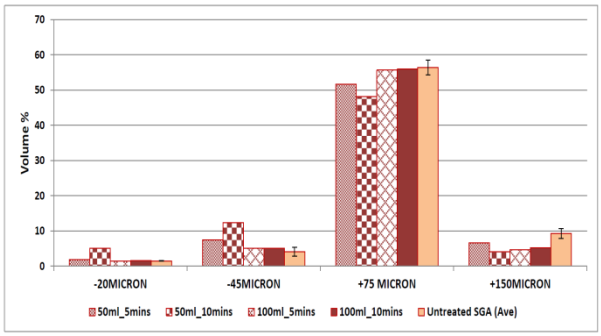

Figure 8. Particle size distribution of sonicated standard SGA compared to untreated SGA

4.3 The Case of Laboratory Calcined Alpha Alumina

Fused alpha alumina, in the form of corundum or sapphire for example is generally known to be a very hard material exhibiting a hardness of 9 on the Mohs hardness scale. However, the fully calcined alpha alumina produced from Bayer gibbsite studied in this work was discovered to be very weak. This was highlighted by the non-ideal force-displacement curves obtained during nanoindentation as discussed in the earlier section and the very low 'apparent' hardness measured (not reported).

During sonication treatment, fully calcined alpha alumina was also observed to be very fragile. The difference in particle size distribution of treated and untreated alpha alumina particles is presented in Figure 9. ESEM images of untreated and treated alpha alumina particles are presented in Figure 10 and 11 respectively.

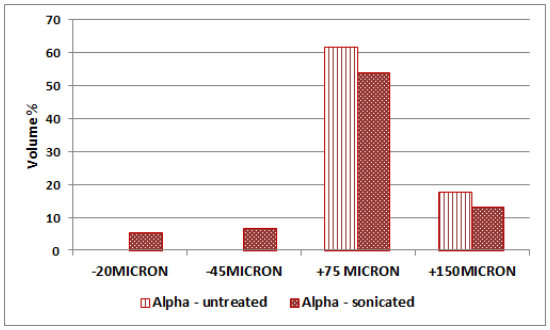

Figure 9. Size distribution of laboratory calcined alpha alumina untreated and sonicated

Figure 10 illustrates the high macro-porosity and the resulting topographically rough surface of the alpha alumina agglomerate observed at very high magnification (x25000). This is consistent

with the cross section presented in Figure 3. These results clearly demonstrate the importance of microstructure on the strength/hardness of these types of materials. This microstructure develops as a result of the de-hydroxylation process where the structural hydroxlys are lost from in between Al-O layers and the layers sinter together in three-dimensions (Metson et al. 2006). This further confirms the reason for the non-ideal curves observed in nanoindentation and the corresponding low hardness.

Some attrition (most likely due to handling) of the untreated alpha alumina was also apparent by the roughness along the aggregate edge (shown in white in Figure 10). Figure 11 demonstrate the type of '*attrition*' cause by sonication which further reveals the rough layered structure of the laboratory calcined alpha alumina.

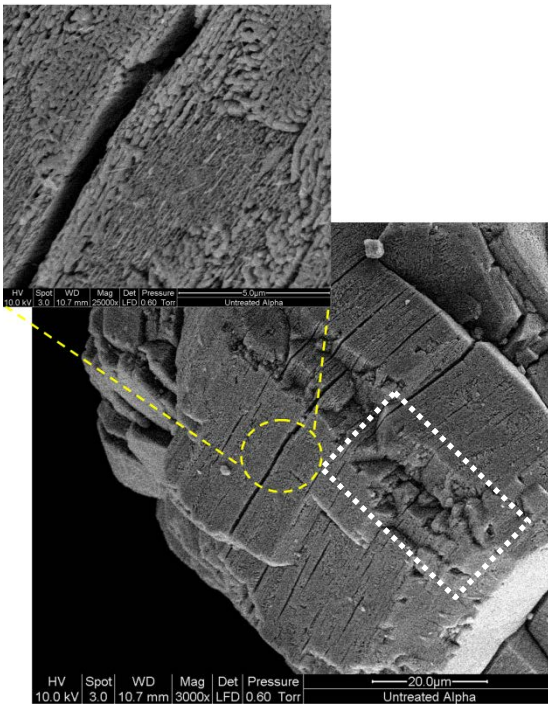

Figure 10. Untreated laboratory calcined alpha alumina showing macro-porous structure at high magnification as well as some attrition due to handling

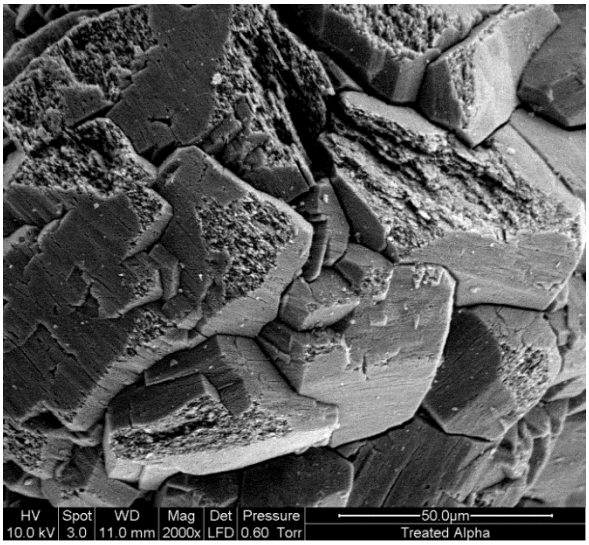

Figure 11. Treated laboratory calcined alpha alumina particle clearly showing particle deterioration due to sonication

5. CONCLUSIONS

Nanoindentation is a powerful technique that can be used to gain mechanical property information of SGA at a very small scale. Results obtained from nanoindentation of alumina need to be interpreted with care due to different non-ideal behaviour that maybe observed depending on the phases present in the sample (i.e. gibbsite, alpha alumina) and crystallite orientation. In such cases, comparison of stiffness or the slope of the unloading force-displacement curve is most suitable.

Nanoindentation testing of three industrial SGAs with different known attrition indices result in comparable mechanical property data. This exemplifies the issue of attrition index not being a reliable measure of particle strength for comparison with more fundamental mechanical properties such as stiffness, modulus and hardness.

Particle breakage induced using ultrasound is an established phenomenon that can be applied for the purposes of studying alumina breakage. Preliminary work conducted demonstrates that this is a relatively simple technique to carry out with the outcome of reasonably quantifiable particle breakage. Laboratory calcined alpha alumina has been demonstrated to have broken down significantly due to sonication which highlights its fragile nature that was also observed by nanoindentation.

Thus nanoindentation and ultrasound mediated particle breakage testing are complimentary techniques that can be used to progress towards defining what *should be* meant by alumina strength which is both fundamental as well as industrially relevant. Furthermore these techniques used together with other powerful tools such as ESEM and TEM; have the potential to provide valuable insights into the relationship between strength and microstructure.

6. ACKNOWLEDGEMENT

We sincerely acknowledge Outotec for sponsoring this work and providing us with a range of industrial samples for testing.

7. REFERENCES

Audet, D. and R.E. Clegg. *Development of a new attrition Index using single impact*. in *Proceedings of the 8th International Alumina Quality Workshop*. 2008.

Anjier, J.L. and D.F.G. Marten, *Particle Strength of Bayer Hydrate*, in *Light Metals*, J.E. Andersen, Editor 1982, TMS

Bradby, J. E., et al. *Mechanical deformation of InP and GaAs by spherical indentation.,* Applied Physics Letters, vol. 78, no. 21, pp. 3235, 2001.

Coghill, P.J. and P. Giang, *Ultrasonic velocity measurements in powders and their relationship to strength in particles formed by agglomeration.* Powder Technology, 2011. **208**: pp. 694-701.

Coghill, P.J. and P.M. Giang, *Measurement of particle strength in alumina powders using ultrasound*, in *Proceedings of the 8th Alumina Quality Workshop* 2008.

Chandrashekar, S., et al. *Alumina Fines' Journey from Cradle to Grave*. in *Proceedings of the 7th International Alumina Quality Workshop*. 2005.

Clerin, P. and V. Laurent., *Alumina Particle Breakage in Attrition Test*. in *Light Metals*. 2001. TMS.

Dickinson, M.E. and J.P. Schirer, *Probing more than the surface.* Materials Today, 2009. **12**(7-8): pp. 46-50.

Ilievski, D., et al. *Quantifying the breakage behaviour of alumina samples*. in *Proceedings of the 7th international alumina quality workshop*. 2005

Kippax, P., *Measuring particle using modern laser diffraction techniques.* Paint and Coatings Industry Magazine, 2005(August)

Kass, M.D., *Ultrasonically induced fragmentation and strain in alumina particles.* Materials Letters, 2000. **42**: pp. 246-250.

Kelchner, C., et al. *Dislocation nucleation and defect structure during surface indentation*. Physical Review B, vol. 58, pp. 11085-11088, Nov. 1998

Kusters, K.A., et al., *Ultrasonic fragmentation of agglomerate powders.* Chemical Engineering Science, 1993. **48**(24): pp. 4119-4129.

Metson, J., et al. *Evolution of Microstructure and Properties of SGA with Calcination of Bayer Gibbsite*. in *Light Metals* 2006. TMS.

Malvern, *Mastersizer 2000 - User Manual*.

Oyen, M.L. and R.F. Cook, *A practical guide for analysi of nanoindentation data.* Journal of Mechanical Behavior of Biomedical Materials 2009. **2**(4): pp. 396-407

Oliver, W.C. and G.M. Pharr, *Measurement of hardness and elastic modulus by instrumented indentation: Advances in understanding and refinements to methodology.* Journal of Materials Research, 2004. **19**(1): pp. 3-20

Oliver, W.C. and G.M. Pharr, *An improved technique for determining hardness and elastic modulus using load and displacement sesing indentation experiments.* Journal of Materials Research, 1992. **7**(6): pp. 1564-1583

Perander, L.M., et al., *Two Perspectives on the Evolution and Future of Alumina*, in *Light Metals*, S.J. Lindsay, Editor 2011, TMS: San Diego.

Sang, J.V., *Factors Affecting the Attrition Strength of Alumina Products*, in *Essential Readings in Light Metals* 2013, John Wiley & Sons, Inc. pp. 740-746.

Scholz, T., et al., *Fracture toughness from submicron derived indentation cracks*, Appl. Phys. Lett. 84, 3055 (2004)

Stählin, W., et al., *Alumina Morphology and Particle Strength*, in *Light Metals*1985, TMS.

Yamada, K., et al., *Development of Fluid Calciner with Suspension Preheaters*, in *Light Metals* 1983, TMS.